A Bayesian Model to Estimate Male and Female Fertility Patterns at a Subnational Level

Riccardo Omenti[1,*], Monica Alexander[2,3], and Nicola Barban[1]

[1] *Department of Statistical Sciences, University of Bologna*

[2] *Department of Statistical Sciences, University of Toronto*

[3] *Department of Sociology, University of Toronto*

[*] *Corresponding email:* `riccardo.omenti2@unibo.it`

September 2024

Abstract

Accurate subnational fertility estimates are crucial for shaping policy decisions across diverse sectors, including education, health care, and social welfare. One of the major challenges in producing these estimates is the presence of small populations, in which information about birth counts stratified by the age at childbearing and fatherhood may be lacking or inadequate. In this research paper, we describe a Bayesian model tailored to estimate the period Total Fertility Rates (TFR) for both men and women at a subnational level. Building on previous work by Schmertmann and Hauer (2019), the model utilizes population counts from age-sex pyramids and models age-specific mortality and fertility patterns accounting for uncertainty and allowing for spatial and temporal dependencies. Testing the model with simulated data that mimic Australian regions, as well as with real data from US counties, demonstrates its ability to generate reasonable TFR estimates. The proposed model exhibits significant potential for the examination of male and female fertility behaviors across various subregions and time frames in multiple countries.

1 Introduction

Precise subnational fertility estimates represent an essential tool for analyzing shifts in fertility patterns within a country. Reliable subnational fertility estimates help researchers to identify compositional and contextual factors influencing fertility behaviors at a local level.

This research paper emphasizes the importance of examining not only among women fertility but among men at a subnational level. While female fertility has been well-documented globally, male fertility tend to be neglected due to a significant lack of high quality information (Coleman (1995)). This bias mirrors the focus on female fertility in data collection efforts. Collecting data on the fertility behavior of women is comparatively easier due to a more precise definition of the childbearing age interval and the superior information quality in surveys (Greene and Biddlecom (2000)). Nonetheless, confining fertility studies exclusively to women lead researchers to neglect the distinctive aspects associated with fertility behaviors among men (Schoumaker, 2019).

Previous studies (Dudel and Klüsener, 2016; Ratcliffe et al., 2000; Keilman et al., 2014; Schoumaker, 2017; Schmertmann and Hauer, 2019; Dudel et al., 2023; Zhang, 2010; Paget and Timæus, 1994; Schoumaker, 2019) have documented substantial differences between male and female fertility. In general, the age-specific fertility curves of men have been found to be somewhat similar to that of women. However, unlike women, men typically have a broader reproductive age span, with lower age-specific fertility at younger ages and higher levels at older ages (Schoumaker, 2019). In addition, non-negligible disparities in the total fertility rate (TFR) by sex have been found (Schoumaker, 2019; Dudel and Klüsener, 2016; Zhang, 2010; Schoumaker, 2017; Ratcliffe et al., 2000) . In low-fertility settings, fertility levels among men and women tend to be similar, with female fertility being slightly higher than that male fertility (Dudel and Klüsener (2016); Zhang (2010)). Conversely, in high-fertility settings, especially in polygynous societies, male fertility have been shown to be disproportionately higher than female fertility (Tragaki and Bagavos (2014); Schoumaker (2017, 2019)). In the context of developing countries, Schoumaker (2019) found that higher differences between male and female fertility are associated with the prevalence of polygynous unions and with greater disparities between age at childbearing and age at fatherhood. In addition to polygyny and differences in paternal ages, sex ratio imbalances have been found to be major drivers of the observed differences between male and female fertility. For instance, Dudel and Klüsener (2016) found that male fertility was much lower than female fertility in eastern Germany during the 1990s, due to a high proportion of female out-migrants after the fall of the Soviet Union. Similarly, Coleman (1995) documented substantially higher male fertility in France during the 1920s due to the shortage of men following the World War I.

In general, while variations in male and female fertility have been documented at a national level, less attention has been devoted to the study of male and female fertility at a subnational level. One of the main challenges in producing fertility estimates for subnational areas can be attributed to small populations in which variations in birth counts tend to be fairly high. Furthermore, detailed information on births by the age of the parents, especially fathers, is often lacking for subnational populations due to various reasons: data confidentiality concerns, unavailability of paternal information in birth records, low coverage of certain areas within a country, lack of well-functioning vital registration systems, lack of nationally-representative surveys with information on place of residence.

Building on the methodological framework by Schmertmann and Hauer (2019), this research paper aims to propose a Bayesian model for estimating the period TFR across multiple geographical areas without the knowledge of births classified by parental ages. The proposed model allows for the estimation of period TFRs using minimal input data, specifically the number of children aged $0-4$, the number of women in the reproductive age interval $15-49$ and the number of men aged $15-59$. Unlike the original model by Schmertmann and Hauer (2019), which focuses solely on the estimation of female TFRs, our objective is to expand this model in two ways: first, by enabling the estimation male fertility, and second, by accounting for temporal and spatial dependencies among adjacent areas and consecutive years.

To the best of our knowledge, this research paper represents one of the first attempts to develop a Bayesian model for estimating male fertility at a subnational level. Our proposed model relies on a Bayesian hierarchical structure, which allows for the incorporation of prior information about mortality schedules and standard age-specific fertility patterns. In addition, it allows to construct credible intervals for the TFR estimates, helping to understand fertility patterns in smaller geographical areas where uncertainty is higher.

The following section will briefly describe the importance of Bayesian methods in demography.

We then provide a detailed description of the proposed model followed by a short portrayal of the main data sources used for the analysis. Finally, we present the results by fitting the model to simulated data from Australian regions over the period 2001-2020 and to United States county-level population data over the period 1982-2019. A discussion of possible extensions of our model to subpopulations from other countries is also discussed.

1.1 Bayesian Methods in Demography

Bayesian methods have become increasing common in Demography due to their ability of combining multiple data sources in the same model and of accounting for various types of errors. The employment of Bayesian methods has allowed unprecedented advancements in the estimation and forecast of national populations (Raftery et al., 2012, 2014), migration (Bijak et al., 2008; Bijak and Wiśniowski, 2010; Abel et al., 2013), fertility (Alkema et al., 2011; Schmertmann et al., 2014; Ellison et al., 2024) and mortality (Alexander and Alkema, 2018; Raftery et al., 2013; Alkema and New, 2014).

In the context of subnational estimation, Bayesian methods have also been widely used. For subnational mortality, Alexander et al. (2017) and Schmertmann and Gonzaga (2018) developed Bayesian hierarchical models to estimate subnational mortality in contexts where data availability is limited.

Regardining subnational populations, Bayesian methods have again played a crucial role. Bryant and Graham (2013) proposed a formal Bayesian framework to obtain subnational population estimates for six regions in New Zealand relying on multiple data sources. More recently, Alexander and Alkema (2022) developed a Bayesian method to estimate and forecast subnational population estimates by age and sex in contexts with limited data. In addition, the 'digital revolution' has led researchers to produce subnational population estimates from non-traditional data sources within a Bayesian framework. For instance, Leasure et al. (2020) developed Bayesian hierarchical model to obtain subnational population estimates using geo-located data.

Concerning subnational fertility estimation, Ševčíková et al. (2018) proposed a Bayesian model to estimate and forecast subnational TFRs that are consistent with the national estimates produced by the United Nations. Schmertmann et al. (2013) employed empirical Bayesian methods to smooth volatile regional fertility data and then applied a new variant of the Brass relational model.

Despite the unprecedented developments in demographic estimation with Bayesian methods, male fertility estimation has been largely ignored, especially at a subnational level. Building on the methodological framework by Schmertmann and Hauer (2019), we present a Bayesian model to examine the evolution of subnational male and female TFR estimates over time and space. By combining multiple data sources, it allows uncertainty to be incorporated and estimates to be driven by the available data. The proposed model requires the availability of accurate population estimates by age and sex. However, it does not require any knowledge of subnational fertility patterns. We utilize statistical model based on principal components derived from national fertility patterns. To incorporate the mortality experienced by children and their potential parents, our model demands the availability of subnational mortality estimates. Although the latter is a strong requirement, we acknowledge the potential of developing a more complex mortality model to address situations where accurate subnational mortality estimates are not available.

2 Method

2.1 Model Setup

Let $C_{a,t}$ be the observed number of children in area a at time t. We assume that it can be modelled as a Poisson distribution:

$$C_{a,t} | K^{s}_{x,a,t} \sim \text{Pois}\left(\sum_{x=15}^{\omega^{s}} K^{s}_{x,a,t} E^{s}_{x,a,t} \right) \tag{1}$$

where $K^s_{x,a,t}$ is the expected number of children per individual of sex s in the age group x in area a at time t, $E^s_{x,a,t}$ indicates the observed number of individuals of sex s in the age group x in area a at time t, ω^s is the last reproductive age group for individuals of sex s. The latter is assumed to be $45-49$ for women and $55-59$ for men. In addition, throughout this paper, we will consider demographic quantities calculated for five-year age groups.

By harnessing standard approximations from cohort-component projection methods (see Keyfitz et al. (2005) for the mathematical details), we can define $K^s_{x,a,t}$ as follows.

$$K^{s}_{x,a,t} = \left[\frac{L^{s}_{x-5,a,t}}{L^{s}_{x,a,t}} \cdot F^{s}_{x-5,a,t} + F^{s}_{x,a,t} \right] \cdot \frac{L_{0,a,t}}{2} \tag{2}$$

where $L^s_{x,a,t}$ denotes the expected person-years lived by individuals of sex s in age group x in area a at time t. $L_{0,a,t}$ denotes the person-years lived by individuals in the age group $0-4$ in area a at time t. $F^s_{x,a,t}$ denotes the expected fertility experienced by individuals of sex s in the age interval $[x, x+5)$ in area a at time t. We set $F^s_{x,a,t}$ to be zero outside the interval $[15, 60)$ for men and outside the interval $[15, 50)$ for women.

Following Hauer and Schmertmann (2020), we can rearrange equation 2, which can be rewritten as

$$\begin{aligned} K^{s}_{x,t,c} &= TFR^{s}_{a,t} \cdot \frac{L_{0,a,t}}{5} \cdot \frac{1}{2} \left[\frac{L^{s}_{x-5,a,t}}{L^{s}_{x,a,t}} \cdot \phi^{s}_{x-5,a,t} + \phi^{s}_{x,a,t} \right] \\ &= TFR^{s}_{a,t} \cdot \frac{L_{0,a,t}}{5} \cdot p^{s}_{x,a,t} \end{aligned} \tag{3}$$

where $\phi^{s}_{x,a,t} = \frac{5 \cdot F^{s}_{x,a,t}}{TFR^{s}_{a,t}}$ is the fraction of life time fertility occurring to individuals of sex s in the age group x if they are subject to the age-specific fertility rates observed in area a at time t throughout their reproductive ages. $\frac{L_{0,a,t}}{5}$ denotes the expected fraction of still alive among children aged $0-4$ in area a at time t. $TFR^s_{a,t}$ is the period Total Fertility Rates experienced by either men or women in area a at time t. This demographic measure can be interpreted as the expected number of children per man (woman) in area a at time t if he (she) is subject to the current period age-specific fertility rates throughout his (her) reproductive ages. $p^{s}_{x,a,t}$ can be defined as an average of the life-time fertility experienced by either men or women in the age groups x and $x-5$. Note that we are assuming that fertility does not begin until age 15; hence, we set $\phi^s_{10,a,t} = 0$.

Equation 3 decomposes the expected number children per man (woman) in age group x in area a at time t as a product of three multiplicative factors. The first two factors, i.e., $TFR^s_{a,t}$ and $\frac{L_{0,a,t}}{5}$, remain constant across the reproductive age groups, while the third factor $p^{s}_{x,a,t}$ varies with age.

Our proposed Bayesian model 3 incorporates demographic knowledge and uncertainty about demographic quantities by placing models and priors on mortality and fertility parameters in equation 2.

2.2 Model for Age-specific Fertility

To incorporate prior knowledge about age fertility schedules, we model the share of life time fertility in a age group x on the log scale as

$$\gamma^s_{x,a,t} = m^s_x + y^s_{1,x}\beta^s_{1,a,t} + y^s_{2,x}\beta^s_{2,a,t} + \nu^s_a + \delta^s_t + \epsilon^s_{a,t} \tag{4}$$

where $\gamma^s_{x,a,t} = \log\left(\frac{\phi^s_{x,a,t}}{\phi^s_{15,a,t}}\right)$ is an index defined as the log transformation of the ratio of the share of life time fertility in age group x to the share of life time fertility in age group $15-19$. The transformation of $\phi^s_{x,a,t}$ ensures that $\gamma^s_{x,a,t}$ on the right hand-side of equation 4 can assume both positive and negative values.

$\boldsymbol{m}^s$, $\boldsymbol{y}^s_1$ and $\boldsymbol{y}^s_2$ are components derived from a set of standard age-specific fertility curves. In particular, $\boldsymbol{m}^s$ is a vector containing the age-specific means of the log-transformed fertility schedules ($\gamma^s_{x,a,t}$), while $\boldsymbol{y}^s_1$ and $\boldsymbol{y}^s_2$ are the first and second left-singular vectors which are obtained via a Singular Value Decomposition on the matrix $\boldsymbol{Y}^s$ whose columns are log-transformed male (female) age-specific fertility schedules.

For example, in our application to US counties we employ the US national age-specific female fertility curves for the historical period $1982-2021$ retrieved from the Human Fertility Database (Jasilioniene et al. (2015)). US national age-specific male fertility schedules are derived from the Human Fertility Collection (Grigorieva et al. (2015)) and cover the historical period $1982-2015$.

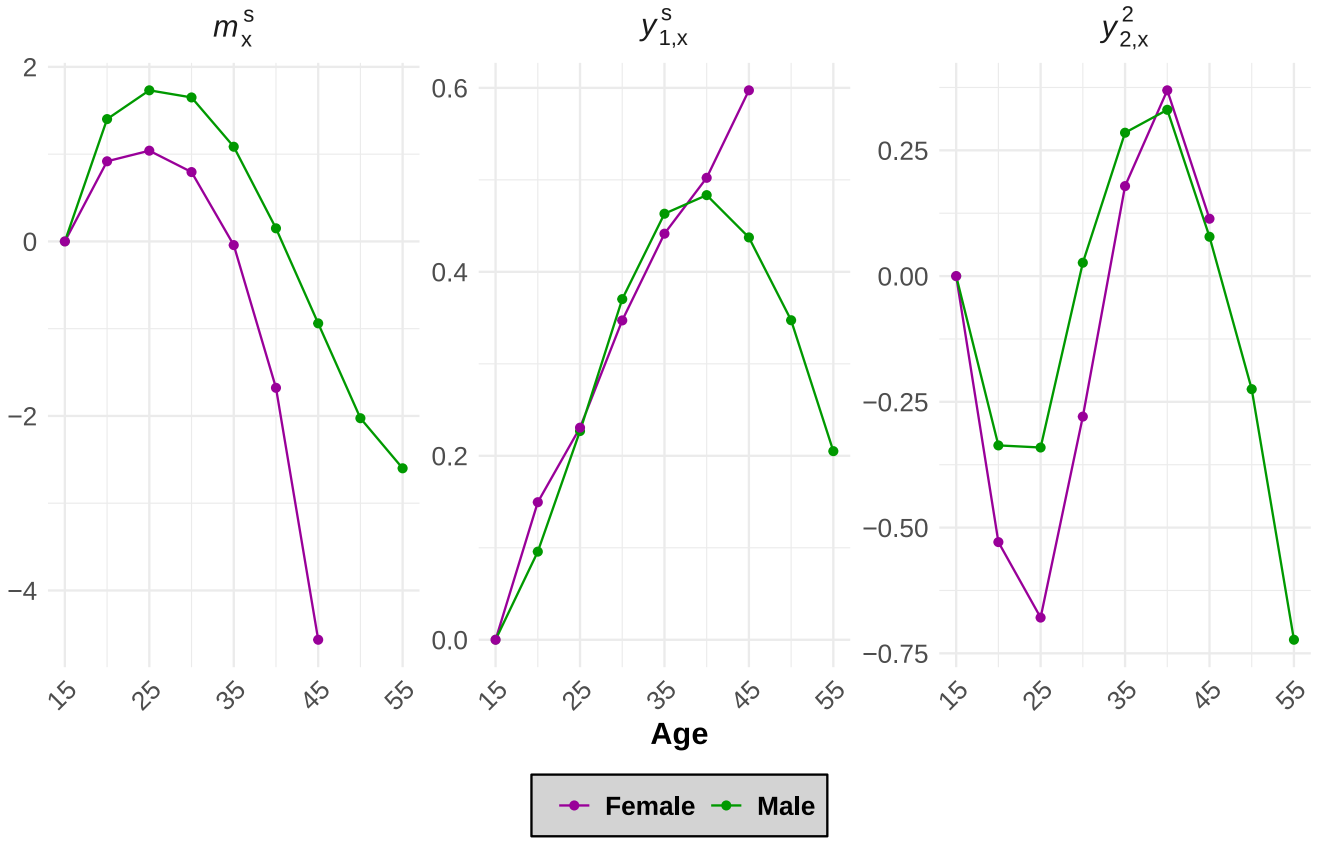

Figure 1: The figure provides an example of the Principal Component Analysis applied to logged U.S. age- and sex-specific fertility proportions ($\gamma^s_{x,a,t}$). The first plot illustrates the average logged fertility rates proportions across the distinct reproductive age classes by sex ($\mathbf{m}^s$). The second and third plots display the values of the first ($\boldsymbol{y}^s_1$) and second ($\boldsymbol{y}^s_2$) left-singular vectors of the matrix ($\boldsymbol{Y}^s$) separately for men and women.

The mean $\boldsymbol{m}^s$ describes the overall age-specific fertility curve. As expected, both male and female age-specific fertility patterns increase up to the age $30-34$ and then start to taper off. The decrease is substantially faster for women compared to men due the narrower female reproductive age span. For both men and women, the first principal component seems to allow for the postponement of the mean age at parenthood, strictly increasing for women throughout the reproductive age period and for men up to the age class $40-44$. This is coherent with the 'postponement transition' suggested by Kohler et al. (2002). The second principal component allows for higher fertility levels in the reproductive age interval $35-44$. For instance, in regions with a high share of highly educated men and women in reproductive ages, fertility in the age interval $35-44$ may be higher than the mean age fertility pattern.

$\beta^s_{1,a,t}$ and $\beta^s_{2,a,t}$ are defined as shape parameters drawn independently from a standard normal distribution for each combination of area a, sex s and time t.

$$\beta^{s}_{p,a,t} \sim \mathcal{N}(0,1) \tag{5}$$

The parameters ν^{s}_{a} controls the spatial autocorrelation among neighboring counties. These spatial effects are modelled via a conditionally autoregressive process (CAR) (Besag and Kooperberg, 1995).

$$\nu^{s}_{a} | \nu^{s}_{b} \sim \mathcal{N}\left(\frac{1}{n_{\delta_a}} \cdot \sum_{b \in \delta_a} w_{a,b} \nu^{s}_{a}, n_{\delta_a} \lambda^{s}_{\nu}\right) \tag{6}$$

where $w_{a,b}$ is a weight being equal to 1 if county b is a neighbor of county a or 0 otherwise. δ_a indicates the set of neighbors for county a. n_{δ_a} denotes the number of neighbors of county a. λ^s_ν is the precision of the spatial effect ν^{s}_{a}. Following the suggestions by Knorr-Held (2000), we assign to λ^s_ν a gamma with parameters equal to 2 and 0.01. Namely,

$$\lambda^{s}_{\nu} \sim \text{gamma}(2, 0.01) \tag{7}$$

The parameter δ^{s}_{t} accounts for the temporal dependence of age-specific fertility patterns between consecutive years. This temporal effect is modelled via a first-order random walk. Specifically, this allows the observed temporal effect for a given year to depend on that of the previous year.

$$\delta^{s}_{t} \sim \mathcal{N}(\delta^{s}_{t-1}, \sigma^2_\delta) \tag{8}$$

The parameter $\epsilon^s_{a,t}$ captures the residual spatio-temporal autocorrelation that is not accounted by the other indepedent spatial and temporal effects. It is assigned a normal distribution with zero mean.

$$\epsilon^s_{a,t} \sim \mathcal{N}(0, \sigma^2_\epsilon) \tag{9}$$

We place weakly informative priors on the standard deviation parameters σ_δ and σ_ϵ.

$$\sigma_\delta \sim \mathcal{N}^{+}(0,1) \tag{10}$$

$$\sigma_\epsilon \sim \mathcal{N}^{+}(0,1) \tag{11}$$

By simulating age-specific proportions of life-time fertility (see figure 2) for six hypothetical regions over a 10-year time window, we are able to capture a wide variety of age-specific fertility patterns. In order to obtain the trajectories in figure 2, we generated values for the model parameters according to the probability distributions specified above and employed the simulated values of the parameters to obtain numerical values for $\gamma^{s}_{x,a,t}$. The simulated numerical values for $\phi^{s}_{x,a,t}$ can be obtained by applying the following transformation to the simulated values of $\gamma^{s}_{x,a,t}$.

$$\phi^{s}_{x,a,t} = \frac{\exp\left(\gamma^{s}_{x,a,t}\right)}{\sum\limits_{x=15}^{\omega^{s}} \exp\left(\gamma^{s}_{x,a,t}\right)} \tag{12}$$

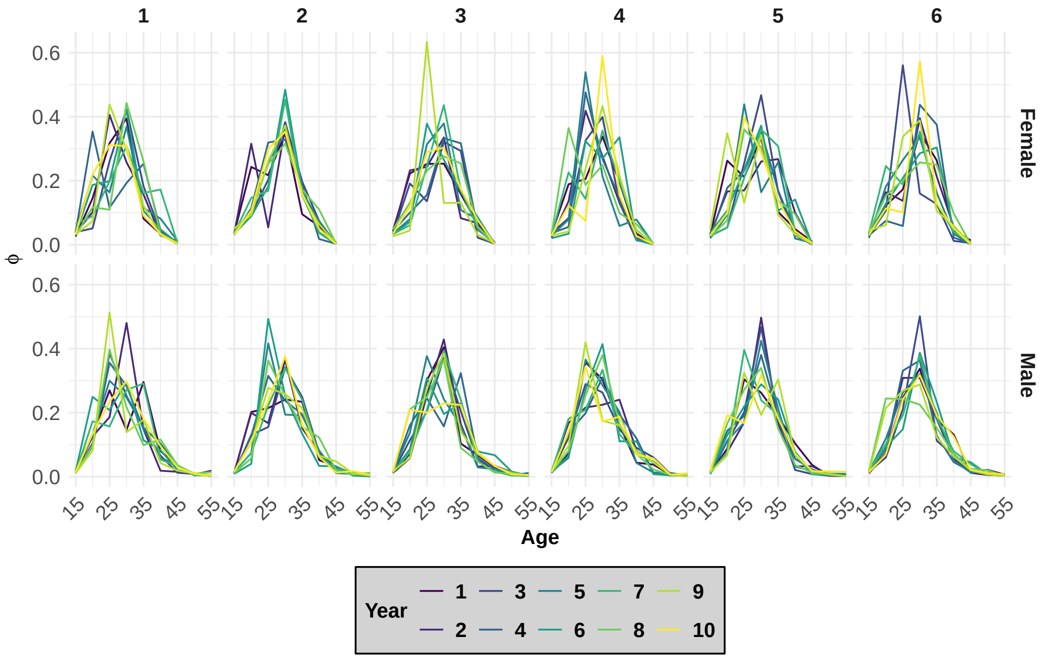

Figure 2: The figure illustrates simulated age-specific fertility proportions ($\phi^{s}_{x,a,t}$) for both women and men from 6 hypothetical regions over a 10-year period.

2.3 Priors on Total Fertility Rates

The Total fertility rate $TFR^{s}_{t,a}$ from equation 3 is modelled through a normal distribution, whose mean is assumed to be equal to the national Total Fertility Rate observed at time t ($TFR^{nat,s}_{t}$) for either men or women.

$$TFR^{s}_{t,a} \sim \mathcal{N}(TFR^{state,s}_{t}, \sigma^{2}_{TFR^{s}_{t,a}}) \tag{13}$$

The standard deviation parameter $\sigma_{TFR^{s}_{t,a}}$ is assigned a weakly informative prior.

$$\sigma_{TFR^{s}_{t,a}} \sim \mathcal{N}^{+}(0,1) \tag{14}$$

The practical implication of centering the prior distribution of $TFR^{s}_{t,a}$ to the state value $TFR^{nat,s}_{t}$ is to shrink counties with a small population towards the state average. In this manner, fertility levels in small counties are partially informed by the state fertility level. On the contrary, fertility levels in larger counties are primarily determined by their population age-sex structure. In addition, if state-level TFR values are unavailable, we center the distribution of the TFR parameter around the national average. In our example, US male TFR values are available until 2004 at the state level. Therefore, from 2004, we let the mean of TFR parameters for men be equal to the national value.

2.4 Priors on Mortality Parameters

Schmertmann and Hauer (2019) modelled child and adult mortality with the log-quadratic mortality model by Wilmoth et al. (2012). Without delving into technical details, they established prior distributions for the two parameters of the log-quadratic model by Wilmoth et al. (2012) and recovered the age-specific Person-Years using standard life table relationships.

Our proposed model incorporates information about child and adult mortality by placing a prior probability distribution directly on the person-years parameters ($L_{0,a,t}$ and $L^{s}_{x,a,t}$) of equation 3. Specifically, we can take advantage of the availability of US subnational life table estimates. In our data example, we used county-specific life tables for the historical period $1982 - 2019$ from the US Mortality Database (visit website usa.mortality.org for downloading the data and see Alexander et al. (2017) for the methodological details). However, we acknowledge that the direct modelling of the Person-Years is feasible provided that subnational mortality life tables are available for the country of interest. In case we lack detailed subregional mortality data, we can resort to other mortality models such as the log-quadratic model that only requires the knowledge of child mortality.

Operationally, in order to include the uncertainty associated to the subnational Person-Years estimates in 3, we assume that the Person-Years $L^{s}_{x,a,t}$ for individuals of sex s in an age group x in area a at time t are normally distributed with a mean equal to the corresponding Person-

Years estimate for the age group x from the subnational life table data referring to sex s, area a and, time t. The variance is calculated through empirical simulations. More details are included in the appendix.

$$\tilde{L}_{0,a,t} \sim \mathcal{N}\left(\hat{L}_{0,a,t}, \hat{\sigma}^2_{\hat{L}_{0,a,t}}\right) \tag{15}$$

$$\tilde{L}^s_{x,a,t} \sim \mathcal{N}\left(\hat{L}^s_{x,a,t}, \hat{\sigma}^2_{\hat{L}^s_{x,a,t}}\right) \tag{16}$$

where $\hat{L}_{0,a,t}$ indicates the estimated Person-Years for the age-group $0-4$ from a period life table constructed using mortality rates observed in area a at time t. $\hat{\sigma}^2_{\hat{L}_{0,a,t}}$ is the corresponding variance calculated by means of simulations. This parameter is included to incorporate information about child mortality. Similarly, $\hat{L}^s_{x,a,t}$ denotes the estimated sex-specific Person-Years for the age classes $x = 10, 15, \ldots, 45$ for women and $x = 10, 15, \ldots, 55$ for men. Such estimates are obtained from a sex-specific subnational life table referring to area a and time t. $\hat{\sigma}^2_{\hat{L}^s_{x,a,t}}$ is the corresponding variance of the estimates.

2.5 Model summary

The model is applied separately for men and women. The following set of equations summarizes the whole model set up. The number of children aged $0-4$ are assumed to be Poisson-distributed (equation 17). The fertility and mortality parameters that govern the Poisson-process (equation 18) are specified by imposing a hierarchical structure. Preliminary information about the overall fertility level is included by placing a probability distribution on the parameter $TFR^s_{t,a}$ (equation 26) and on its standard deviation $\sigma_{TFR^s_{t,a}}$(equation 27). Prior knowledge about the age-specific fertility patterns is incorporated by specifying a statistical model 19 on national age-specific fertility patterns and probability distributions on its parameters. Finally, we include prior knowledge about child and adult mortality by placing a prior probability distributions directly on the person-years parameters (28 and 29).

$$C_{a,t}|K^{s}_{x,a,t} \sim \text{Pois}\left(\sum_{x=15}^{\omega^s} K^{s}_{x,a,t} E^{s}_{x,a,t}\right) \tag{17}$$

$$K^{s}_{x,a,t} = TFR^{s}_{a,t} \cdot \frac{L_{0,a,t}}{5} \cdot \frac{1}{2}\left[\frac{L^{s}_{x-5,a,t}}{L^{s}_{x,a,t}} \cdot \phi^{s}_{x-5,a,t} + \phi^{s}_{x,a,t}\right] \tag{18}$$

$$\gamma^{s}_{x,a,t} = m^{s}_{x} + y^{s}_{1,x}\beta^{s}_{1,a,t} + y^{s}_{2,x}\beta^{s}_{2,a,t} + \nu^{s}_{a} + \delta^{s}_{t} + \tau^{s}_{a,t} \tag{19}$$

$$\phi^{s}_{x,a,t} = \frac{\exp\left(\gamma^{s}_{x,a,t}\right)}{\sum\limits_{x=15}^{\omega^s} \exp\left(\gamma^{s}_{x,a,t}\right)} \tag{20}$$

$$\beta^{s}_{1,a,t}, \beta^{s}_{2,a,t} \sim \mathcal{N}(0,1) \tag{21}$$

$$\nu^{s}_{a}|\nu^{s}_{b} \sim \mathcal{N}\left(\frac{1}{n_{\delta_a}} \cdot \sum_{b\in\delta_a} w_{a,b}\nu^{s}_{a}, n_{\delta_a}\lambda^{s}_{\nu}\right) \tag{22}$$

$$\lambda^{s}_{\nu} \sim \text{gamma}(2, 0.01) \tag{23}$$

$$\delta^{s}_{t} \sim \mathcal{N}(\delta^{s}_{t-1}, \sigma^2_{\delta}) \tag{24}$$

$$\epsilon^{s}_{a,t} \sim \mathcal{N}(0, \sigma^2_{\epsilon}) \tag{25}$$

$$TFR^{s}_{t,a} \sim \mathcal{N}(TFR^{nat,s}_{t}, \sigma^{2}_{TFR^{s}_{t,a}}) \tag{26}$$

$$\sigma_{TFR^{s}_{t,a}}, \sigma_{\epsilon}, \sigma_{\delta} \sim \mathcal{N}^{+}(0,1) \tag{27}$$

$$\tilde{L}_{0,a,t} \sim \mathcal{N}\left(\hat{L}_{0,a,t}, \hat{\sigma}^2_{\hat{L}_{0,a,t}}\right) \tag{28}$$

$$\tilde{L}^s_{x,a,t} \sim \mathcal{N}\left(\hat{L}^s_{x,a,t}, \hat{\sigma}^2_{\hat{L}^s_{x,a,t}}\right) \tag{29}$$

The subscript s refers to sex, the subscript t refers to time and the subscript a denotes the area. The subscript x denotes the age with ω^s being the last reproductive age group. ω^s is set to be $45 - 49$ for women and $55 - 59$ for men.

2.6 Model implementation

Our final goal is to draw sample from the posterior distribution of the $TFR^s_{a,t}$ in an area a at time t conditional on the observed number of children aged 0-4 $C_{a,t}$, the counts of men (women) $E^s_{15,a,t}, \dots, E^s_{\omega^s,a,t}$ and the other model parameters.

Operationally, posterior samples for the TFR parameters were obtained using the statistical R package *nimble* (de Valpine et al., 2017). This package allows to specify the main structure of our model in R, compiles the model in C++ and implement an adaptive Metropolis- within-Gibbs MCMC algorithm to simulate from the posterior distribution of the TFR parameters. Best estimates of the TFR parameters were taken to be the medians of the corresponding posterior samples. 95% credible intervals for the TFR parameters were constructed by computing the 2.5% and 97.5% quantiles from the relevant posterior samples.

3 Data

3.1 Mortality

To account for the mortality of parents and children, we model directly the age-specific person-years. Person-years is a common life table function capturing the number of years lived between two ages. Our data example refers to the US context that provides a rich set of subnational life tables.

Information on county-level mortality are retrieved from the US Mortality Database. This data source provides life tables by sex for both states ($1969-2020$) and counties ($1982-2019$). Additionally, to account for the uncertainty in the county-level mortality indicators, standard errors for the age-specific death probabilities are provided. Based upon the uncertainty of this life table component, we can easily exploit simulations and life table relationships to obtain uncertainty measures for the person-years.

3.2 Fertility

Neither male nor female age-specific fertility rates are available at a county level. Hence, we rely on age-specific fertility rates from the Human Fertility Database for women (Jasilioniene et al., 2016) and from the Human Fertility Collection for men (Grigorieva et al., 2015). Both of these data sources are used to obtain national male and female TFR values.

TFR estimates at the state level are available for women for the entire study (1982-2019) and for men for the period (1982-2004). The US National Bureau of Economic Research provides birth records with information on the parental ages and on the state where the birth occurred for the period 1982-2004 (visit the website `https://data.nber.org/natality/` for more information). Using the method by Dudel and Klüsener (2016), we can easily obtain male and female TFR estimates for the period $1982-2004$. Concerning the period $2005-2019$, National Center for Health Statistics provides TFR values at the state level for only women. Hence, for the period $2005-2019$, we used as prior information the national male TFR values available from the Human Fertility Collection.

3.3 Population counts by age and sex

Population counts by age and sex are taken from National Cancer Institute, which produces annual population estimates from 1969 on in collaboration with US Census Bureau and the National Center for Health Statistics.

Using these data, we retrieved the number of children under age 5, the number of women in the age group $15-49$ and the number of men aged $15-59$ for the period $1982-2019$ and for all the US counties.

3.4 Population counts by age and sex

4 Results

4.1 Simulated Data

To evaluate the performance of our model, we created a simulated data set of children generated using existing subnational fertility and mortality patterns for eight Australian territories [1]. Given the availability of true subnational fertility and mortality estimates by age and sex for the period $2001-2020$, we computed the number of expected children ($K^s_{x,a,t}$) at each parental age group using equation 2. Afterwards, we simulated the overall number of children ($C^s_{a,t}$) according to the relationship shown in equation 1 and applied our proposed model to the simulated data. The number of potential fathers and mothers were treated as fixed. The dependency structure among regions was specified using an adjacency matrix matching the neighboring structure of Australia.

Figure 3 displays the true and estimated TFRs for the eight Australian regions. The dots indicate the true TFRs and are calculated from national birth register data using standard demographic methods. The solid lines denote the TFR estimates that were obtained by fitting the proposed model to the simulated data. The corresponding 95% credible intervals are displayed via shaded regions. Male and female TFR estimates seem to mirror the TFR values quite closely. In addition, regions with higher populations sizes show lower uncertainty around their estimates. Regions such as Tasmania (TS) and Australian Capital Territory (ACT) with

---

[1] More details on the data used for the simulation are reported in the appendix.

smaller populations exhibit wider credible intervals.

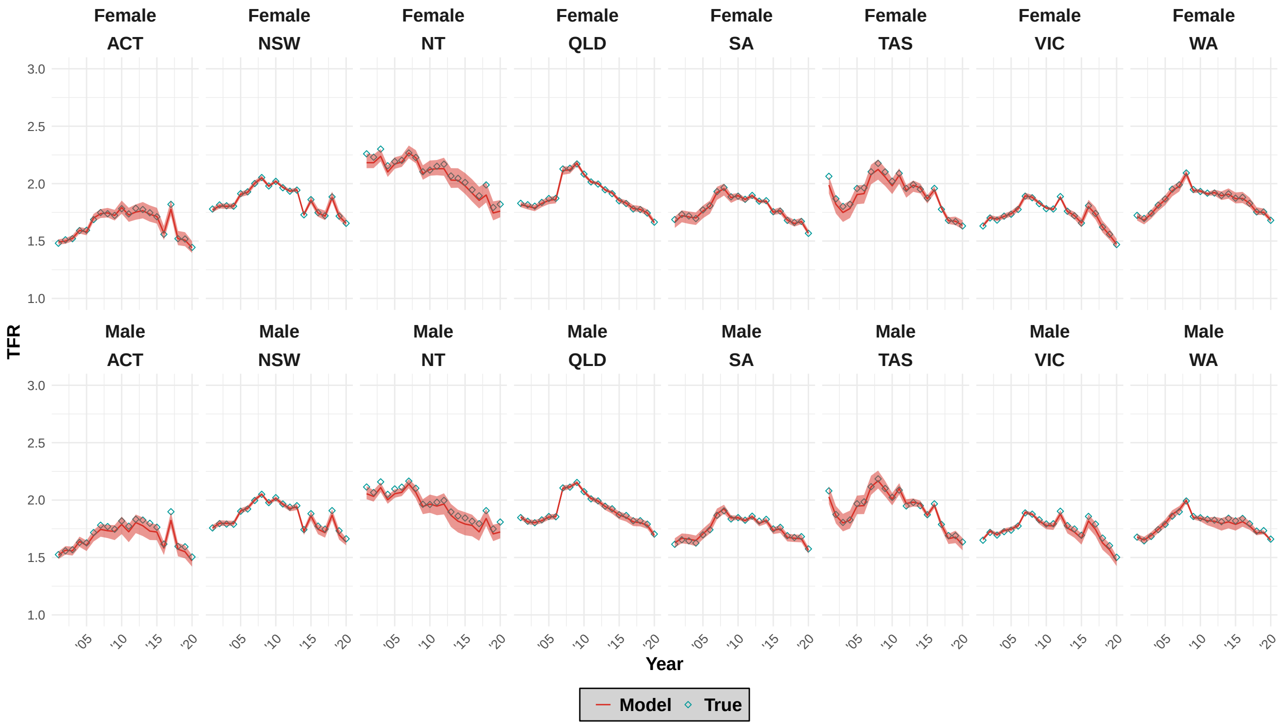

Figure 3: True and simulate total fertility rates for eight territories for the period 2001-2020.

To evaluate the performance of the model, we compare it with the Implied Total Fertility Rate (iTFR) that is obtained via an indirect method by Hauer and Schmertmann (2020).

$$iTFR = \frac{1}{1 - 0.75 \cdot q_{0-4}} \cdot 7 \cdot \frac{C_{0-4}}{W_{15-49}} \tag{30}$$

where q_{0-4} is the probability of death under 5 to account for child survival, C_{0-4} is number of children under 4 and W_{15-49} is the number of potential mothers. The multiplicative constant 7 allows age-specific fertility levels to be equal across the distinct five-year childbearing ages, namely $15 - 19, \ldots, 45 - 49$. By replacing W_{15-49} with the number of men aged $15 - 60$ and the multiplicative constant with 9, we can produce a male version of the iTFR indicator.

For each region, we compare these methods of estimation using the root mean squared error (RMSE), defined as

$$RMSE = \sqrt{\frac{1}{T}\left(\sum_{t=1}^{T} T\hat{F}R_{a,t} - TFR^{*}_{a,t}\right)^{2}} \tag{31}$$

where T is the total number of years, $T\hat{F}R_{a,t}$ is the estimated TFR, and $TFR^{*}_{a,t}$ is the true TFR. The results in table 1 are reported in relative terms due to very small values of the RMSE for both methods. The comparison is made by dividing the RMSE of the indirect method by the RMSE of our proposed model. A value larger than 1 denotes a better performance of our model in comparison to the indirect method by Hauer and Schmertmann (2020), whereas a value less than 1 indicates the oppisite situation.

	Male		**Female**	
State	**Model**	**Indirect**	**Model**	**Indirect**
ACT	1.00	4.43	1.00	2.48
NSW	1.00	12.19	1.00	4.03
NT	1.00	3.23	1.00	3.86
SA	1.00	2.52	1.00	5.85
QLD	1.00	4.38	1.00	2.33
TAS	1.00	2.09	1.00	5.17
VIC	1.00	11.36	1.00	3.43
WA	1.00	7.82	1.00	5.18

Table 1: Performance of the proposed model and of the indirect method by Hauer and Schmertmann (2020).

Table 1 shows the superiority of our Bayesian method with relative RMSE being strictly greater than 1.

4.2 Application to US counties

We applied our proposed model to estimate period TFRs by US counties for the historical period 1982 – 2019. As of 2019, there are 3,244 counties in the country, including the states of Alaska and Hawaii. The population sizes of US counties display a significant heterogeinity ranging from counties with over 10 million residents such as Los Angeles to other with less than 100 people.

As a data example, we illustrate the model results for the counties of two US states: California and Utah. The former is the state with highest population in the country, while the latter has been the state with the highest recorded fertility levels until the middle of 2010s.

The model was fitted separately by sex and state.

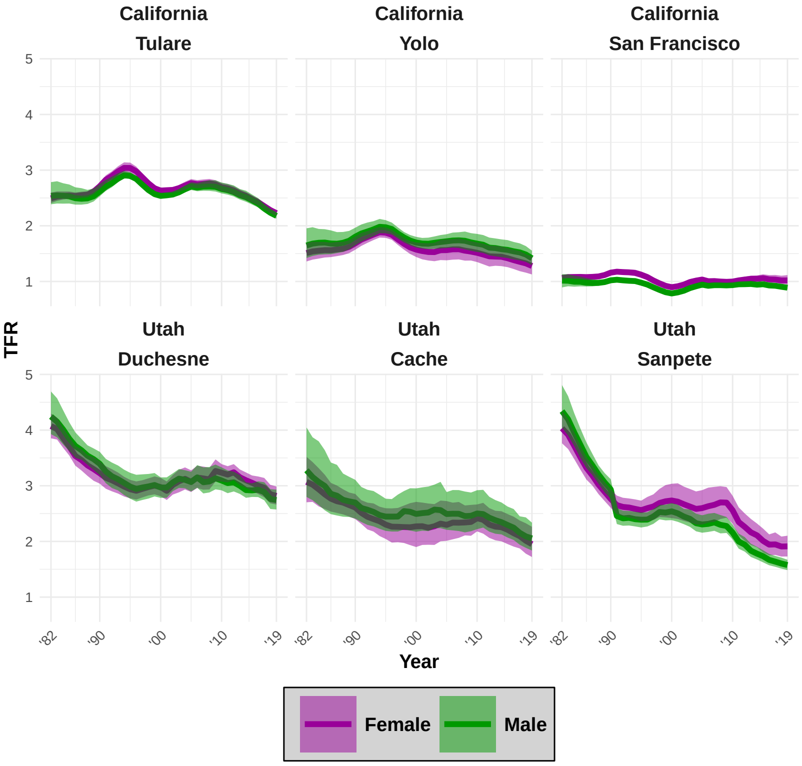

Figure 4: Times series of male and female period TFR estimates for six U.S. counties across the period 1982 – 2019. 95% credible intervals are also provided via shaded areas.

Figure 4 displays the evolution of TFR estimates from 1982 to 2019 of six counties, three in California and three in Utah, disaggragated by sex. TFR estimates are the medians of the corresponding posterior samples.

The California counties, characterized by a higher absolute number of children, display TFR estimates with lower uncertainty compared to counties in Utah. Regarding sex differentials by fertility, we do not observe any staggering difference between men and women. This result is coherent with previous research on male fertility in low-fertility countries (Schoumaker, 2019). Nonetheless, we note that starting from the 1990s female fertility is slightly higher than male fertility. This pattern is coherent with the findings by Dudel and Klüsener (2021), who found a decline in the ratio of male to female TFR at a national level in the United States .

Concerning the temporal evolution of the TFR estimates by sex, we find distinct trajectories in the counties of two states. In California we observed an increase in the TFR estimates for both sexes during the 1990s followed by a decline starting from the 2000s. Previous research

(Johnson and Li, 2007; Hill and Johnson, 2002) attributed this increase to a growing population of young adult migrants from Latin American, who tend to have higher number of children than the US-born population. Tulare County consistently exhibited similar male and female TFR estimates above the replacement level of 2.1 throughout the entire study period. In Yolo, men displayed slightly higher TFR estimates. However, for the majority of the study period, the estimates are below the replacement level. San Francisco showed extremely low fertility levels, with women experiencing being slightly higher fertility than men. This trend may be linked to the high living costs and to a high share of population of working age, who might decide to raise children in more affordable areas.

Counties in Utah experienced a continuous decline in male and female TFRs in the period from 1980s until the early 2000s. Men and women in these counties used to bear on average more than three children thoughout their reproductive period as early as 1982. Nonetheless, in the year 2000, male and female TFR estimates declined by one unit for these Utah counties. Fertility remained roughly constant throughout the period $2000 - 2009$ with values slightly above the replacement level of 2.1. After the year 2009, TFR estimates began to decline again in these Utah counties, possibly as a consequence of the global financial crisis. In this context, both Sanpete and Cache counties reached levels below the replacement levels of 2.1. These implies that, net of migration, the populations of these counties would start to decrease.

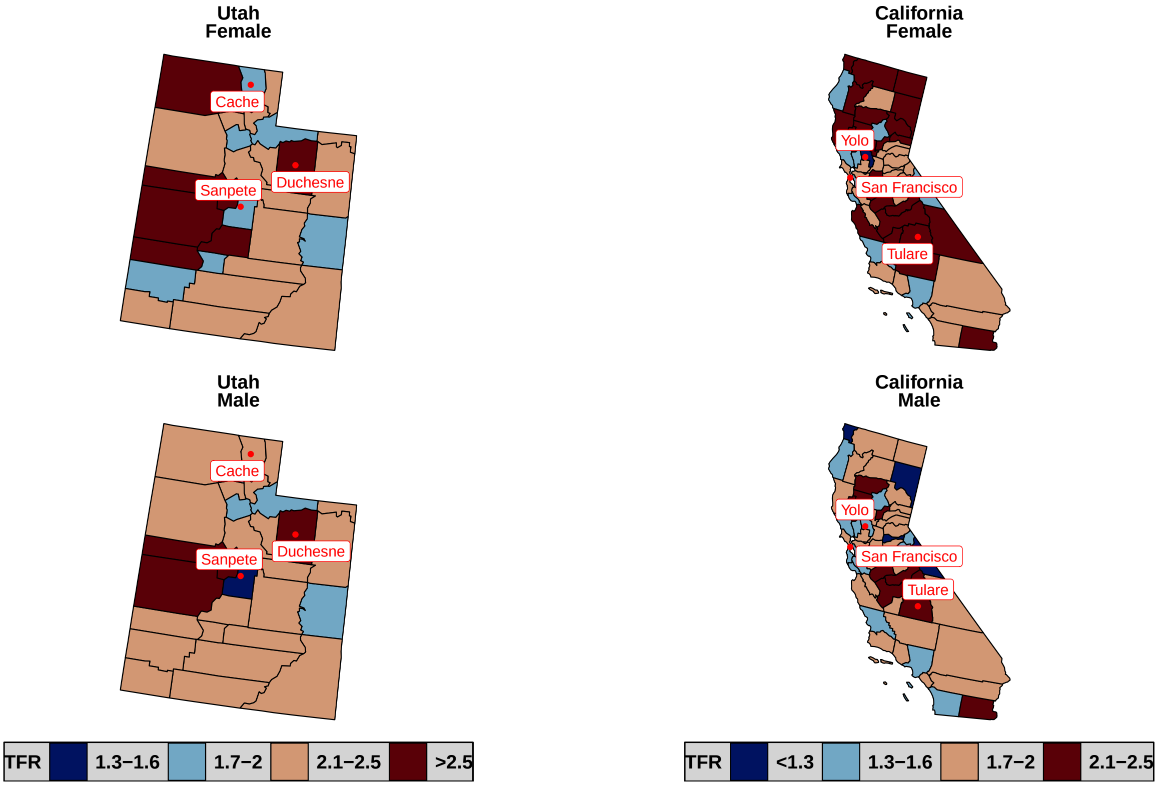

Figure 5: Male and female TFR estimates for Utah and California in 2019.

Figure 5 shows male and female TFR estimates for Utah and California in 2019. TFR estimates are generally higher in Utah compared to California. Most of the Utah counties display a TFR higher than 2.1. Additionally, in both California and Utah counties, women tend to display higher fertility levels than men.

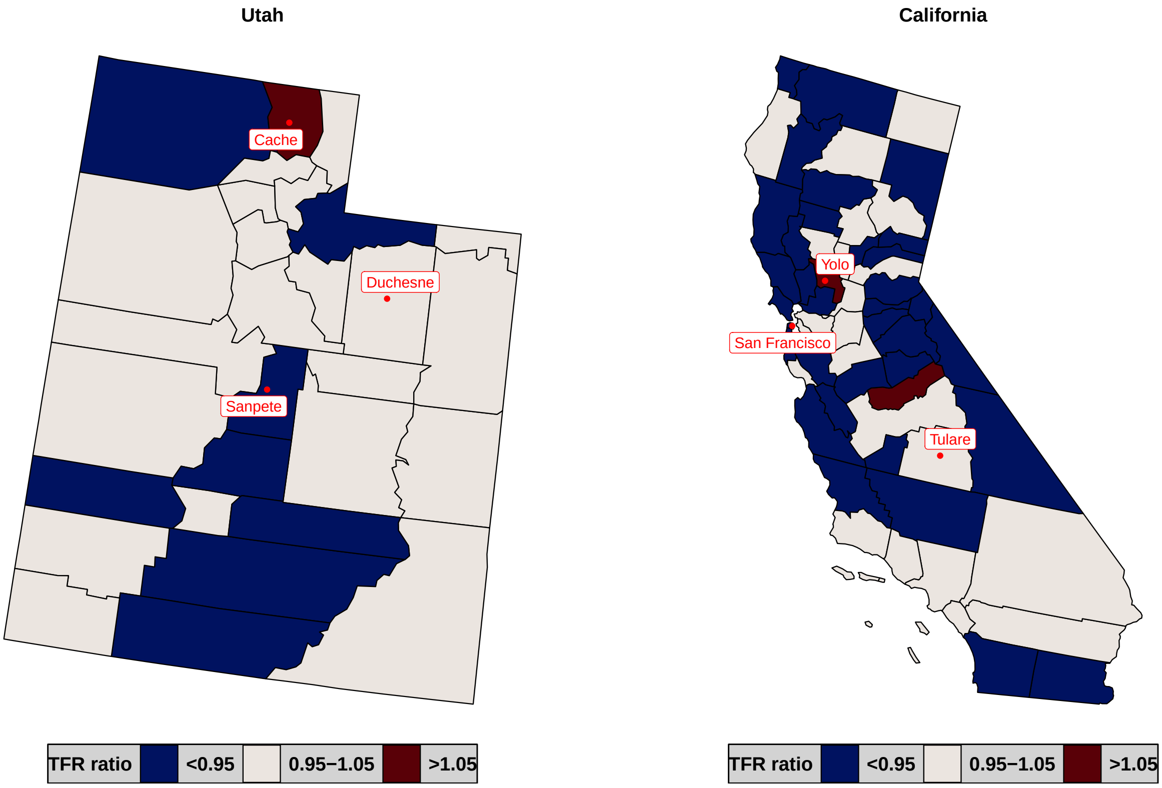

Figure 6: Male to female TFR ratios for Utah and California in 2019.

Figure 6 shows the ratio of the male TFR estimates to the female TFR estimates in 2019 in Utah and California. Overall, the majority of the counties in both states exhibit ratios between 0.95 and 1.05, implying similar levels of fertility between men and women. However, a non-negligiable number of counties display TFR ratios lower than 0.95, with women having an higher average number children compared to men. This is consistent with what has been at national level by Dudel and Klüsener (2021) and at a state level by Schubert and Dudel (2024).

5 Discussion

In this article, we propose a Bayesian modeling framework to estimate subnational TFR for both men and women in situations where the amount of available data limited. The proposed method extends the modeling framework developed by Schmertmann and Hauer (2019) in two ways. First, it allows for the estimation of both male and female fertility. Second, it accounts for possible spatial and temporal dependencies among the units of observation.

When tested with simulated data from regions in Australia, the model outperforms the non-probabilistic indirect estimation by Hauer and Schmertmann (2020). In addition, in comparison to non-probabilistic indirect methods, relying on Bayesian modeling framework enables to quantify the uncertainty around the demographic indicator of interest to the researcher.

After validating the model with simulated data, it was fitted to estimate male and female TFR estimates at the county level in the United States from 1982 to 2019. The results suggest that men and women experience similar fertility patterns across this period, with women exhibiting slightly higher fertility levels than men. The degree of uncertainty around the TFR estimates is linked to the absolute number of children under 5, with higher uncertainty in counties with fewer children. A comparison between Utah and California showed how states within the same country may experience distinct fertility patterns. The majority of counties in Utah displayed TFR estimates above the replacement level of 2.1, whereas only a small portion of counties in California did so.

One of the main advantages of the model is that it does not require any knowledge on the births classified by parental ages - a piece of information only available at a national level in countries with well-functioning data registration systems. Subnational information on births by parental ages is often inaccessible to researchers due to privacy concerns. In countries lacking well-functioning vital registration systems, births classified by parental ages can only be computed from nationally-representative surveys that are not carried out timely due to the high associated costs.

In addition, we argue that our modeling framework can be easily applied to other countries. In most of the developed countries, subnational mortality estimates and subnational population counts by age and sex are made available to researcher without particular restrictions. Concerning developing countries, subnational population estimates by age and sex from the Census Bureau could be leveraged to examine fertility at a subregional level for both males and females. Since the majority of the developing countries lacks subnational mortality estimates, national mortality estimates from United Nations World Population Prospects could be employed and the uncertainty coming from absence of subregional mortality data could be incorporated by placing higher variances on the mortality parameters.

However, we acknowledge that our proposed method model is not free from caveats. First, it relies on the knowledge of national age-specific male fertility patterns, which are only available for only a limited amount of countries. In many countries, especially those without high-quality birth registers, age-specific male fertility rates can only be estimated from nationally-representative surveys such as the Demographic and Health Surveys (DHS). Second, our chosen age range for male reproduction may be overly restrictive for some countries. For example, Schoumaker (2017) showed that in regions such as Sub-Saharan Africa, male age-specific fertility rates can remain above zero until age 75. Third, our model does not properly account for internal migration. For instance, counties with a higher share of college students in comparison to the total population experience temporary population surges in the age classes $15-19$ and $20-24$, which can lead to an underestimation of the actual TFR in these areas.

In conclusion, starting from the methodological framework by Schmertmann and Hauer (2019), the proposed method allows to obtain reliable male and female TFR estimates at a subnational level. The hierarchical Bayesian framework integrates multiple data sources while incorporating their corresponding uncertainty. In addition, in comparison to traditional indirect deterministic methods, our approach offers increased flexibility in modeling fertility processes by accounting for spatial and temporal dependencies.

References

Abel, G., Bijak, J., Findlay, A., McCollum, D., and Wiśniowski, A. (2013). Forecasting environmental migration to the united kingdom: an exploration using bayesian models. *Population and Environment*, 35:183–203.

Alexander, M. and Alkema, L. (2018). Global estimation of neonatal mortality using a bayesian hierarchical splines regression model. *Demographic Research*, 38:335–372.

Alexander, M. and Alkema, L. (2022). A bayesian cohort component projection model to estimate women of reproductive age at the subnational level in data-sparse settings. *Demography*, 59(5):1713–1737.

Alexander, M., Zagheni, E., and Barbieri, M. (2017). A flexible bayesian model for estimating subnational mortality. *Demography*, 54(6):2025–2041.

Alkema, L. and New, J. R. (2014). Global estimation of child mortality using a bayesian b-spline bias-reduction model. *The Annals of Applied Statistics*, pages 2122–2149.

Alkema, L., Raftery, A. E., Gerland, P., Clark, S. J., Pelletier, F., Buettner, T., and Heilig, G. K. (2011). Probabilistic projections of the total fertility rate for all countries. *Demography*, 48(3):815–839.

Besag, J. and Kooperberg, C. (1995). On conditional and intrinsic autoregressions. *Biometrika*, 82(4):733–746.

Bijak, J., Raymer, J., and Willekens, F. (2008). Bayesian methods in international migration forecasting. *International migration in Europe: Data, models and estimates*, pages 255–288.

Bijak, J. and Wiśniowski, A. (2010). Bayesian forecasting of immigration to selected european countries by using expert knowledge. *Journal of the Royal Statistical Society Series A: Statistics in Society*, 173(4):775–796.

Bryant, J. R. and Graham, P. J. (2013). Bayesian demographic accounts: Subnational population estimation using multiple data sources.

Coleman, D. A. (1995). *Male fertility trends in industrial countries: Theories in search of some evidence.* International Union for the Scientific Study of Population.

de Valpine, P., Turek, D., Paciorek, C. J., Anderson-Bergman, C., Lang, D. T., and Bodik, R. (2017). Programming with models: writing statistical algorithms for general model structures with nimble. *Journal of Computational and Graphical Statistics*, 26(2):403–413.

Dudel, C., Cheng, Y.-h. A., and Klüsener, S. (2023). Shifting parental age differences in high-income countries: Insights and implications. *Population and Development Review*, 49(4):879–908.

Dudel, C. and Klüsener, S. (2016). Estimating male fertility in eastern and western germany since 1991: A new lowest low? *Demographic Research*, 35:1549–1560.

Dudel, C. and Klüsener, S. (2021). Male–female fertility differentials across 17 high-income countries: Insights from a new data resource. *European Journal of Population*, 37(2):417–441.

Ellison, J., Berrington, A., Dodd, E., and Forster, J. J. (2024). Combining individual-and population-level data to develop a bayesian parity-specific fertility projection model. *Journal of the Royal Statistical Society Series C: Applied Statistics*, 73(2):275–297.

Greene, M. E. and Biddlecom, A. E. (2000). Absent and problematic men: Demographic accounts of male reproductive roles. *Population and development review*, 26(1):81–115.

Grigorieva, O., Jasilioniene, A., Jdanov, D., Grigoriev, P., Sobotka, T., Zeman, K., and Shkolnikov, V. (2015). Methods protocol for the human fertility collection.

Hauer, M. E. and Schmertmann, C. P. (2020). Population pyramids yield accurate estimates of total fertility rates. *Demography*, 57(1):221–241.

Hill, L. E. and Johnson, H. P. (2002). *Understanding the future of Californians' fertility: the role of immigrants*. Public Policy Instit. of CA.

Jasilioniene, A., Jdanov, D. A., Sobotka, T., Andreev, E. M., Zeman, K., Shkolnikov, V. M., Goldstein, J. R., Philipov, D., and Rodriguez, G. (2015). Methods protocol for the human fertility database. *Rostock: Max Planck Institute for Demographic Research*.

Jasilioniene, A., Sobotka, T., Jdanov, D. A., Zeman, K., Kostova, D., Andreev, E. M., Grigoriev, P., and Shkolnikov, V. M. (2016). Data resource profile: the human fertility database. *International Journal of Epidemiology*, 45(4):1077–1078e.

Johnson, H. P. and Li, Q. (2007). *Birth rates in California*, volume 9. Public Policy Institute of California San Francisco, CA.

Keilman, N., Tymicki, K., and Skirbekk, V. (2014). Measures for human reproduction should be linked to both men and women. *International Journal of Population Research*, 2014(1):908385.

Keyfitz, N., Caswell, H., et al. (2005). *Applied mathematical demography*, volume 47. Springer.

Knorr-Held, L. (2000). Bayesian modelling of inseparable space-time variation in disease risk. *Statistics in medicine*, 19(17-18):2555–2567.

Kohler, H.-P., Billari, F. C., and Ortega, J. A. (2002). The emergence of lowest-low fertility in europe during the 1990s. *Population and development review*, 28(4):641–680.

Leasure, D. R., Jochem, W. C., Weber, E. M., Seaman, V., and Tatem, A. J. (2020). National population mapping from sparse survey data: A hierarchical bayesian modeling framework to account for uncertainty. *Proceedings of the National Academy of Sciences*, 117(39):24173–24179.

Paget, W. J. and Timæus, I. M. (1994). A relational gompertz model of male fertility: Development and assessment. *Population Studies*, 48(2):333–340.

Raftery, A. E., Alkema, L., and Gerland, P. (2014). Bayesian population projections for the united nations. *Statistical science: a review journal of the Institute of Mathematical Statistics*, 29(1):58.

Raftery, A. E., Chunn, J. L., Gerland, P., and Ševčíková, H. (2013). Bayesian probabilistic projections of life expectancy for all countries. *Demography*, 50(3):777–801.

Raftery, A. E., Li, N., Ševčíková, H., Gerland, P., and Heilig, G. K. (2012). Bayesian probabilistic population projections for all countries. *Proceedings of the National Academy of Sciences*, 109(35):13915–13921.

Ratcliffe, A. A., Hill, A. G., and Walraven, G. (2000). Separate lives, different interests: male and female reproduction in the gambia. *Bulletin of the World Health Organization*, 78:570–579.

Schmertmann, C., Zagheni, E., Goldstein, J. R., and Myrskylä, M. (2014). Bayesian forecasting of cohort fertility. *Journal of the American Statistical Association*, 109(506):500–513.

Schmertmann, C. P., Cavenaghi, S. M., Assunção, R. M., and Potter, J. E. (2013). Bayes plus brass: estimating total fertility for many small areas from sparse census data. *Population studies*, 67(3):255–273.

Schmertmann, C. P. and Gonzaga, M. R. (2018). Bayesian estimation of age-specific mortality and life expectancy for small areas with defective vital records. *Demography*, 55:1363–1388.

Schmertmann, C. P. and Hauer, M. E. (2019). Bayesian estimation of total fertility from a population's age–sex structure. *Statistical Modelling*, 19(3):225–247.

Schoumaker, B. (2017). Measuring male fertility rates in developing countries with demographic and health surveys: An assessment of three methods. *Demographic Research*, 36:803–850.

Schoumaker, B. (2019). Male fertility around the world and over time: How different is it from female fertility? *Population and Development Review*, pages 459–487.

Schubert, H.-A. and Dudel, C. (2024). Same but different? male-female fertility differences at the subnational level over time and across countries. In *Paper presented at European Population Conference 2024 in Edinburgh, UK.*

Ševčíková, H., Raftery, A. E., and Gerland, P. (2018). Probabilistic projection of subnational total fertility rates. *Demographic research*, 38:1843.

Tragaki, A. and Bagavos, C. (2014). Male fertility in greece: Trends and differentials by education level and employment status. *Demographic Research*, 31:137–160.

Van der Vaart, A. W. (2000). *Asymptotic statistics*, volume 3. Cambridge university press.

Wilmoth, J., Zureick, S., Canudas-Romo, V., Inoue, M., and Sawyer, C. (2012). A flexible two-dimensional mortality model for use in indirect estimation. *Population studies*, 66(1):1–28.

Zhang, L. (2010). *Male fertility patterns and determinants*, volume 27. Springer Science & Business Media.

Appendix

Variance Estimation for Subnational Mortality Data

In our US example, we use the estimates of the variances of the subnational death probabilities $\overset{s}{\hat{q}}_{x,a,t}$ to estimate the variances of the subnational Person-Years estimates. Specifically, for each combination of age group x, area a, time t and sex s, we transform the reported death probability estimates $(\overset{s}{\hat{q}}_{x,a,t})$ in the logit scale $\text{logit}(\hat{q}^{s}_{x,a,t})$ and simulate the transformed death probabilities from a normal distribution centered around the subnational estimate on the logit scale reported in the life table from the US Mortality Database. We draw a random sample of J logit-transformed death probabilities

$$\text{logit}(q_{0,a,t})^{(j)} \sim \mathcal{N}\left(\text{logit}(\hat{q}_{0,a,t}), \left[\frac{\hat{\sigma}_{q_{0,a,t}}}{\hat{q}_{0,a,t} \cdot (1 - \hat{q}_{0,a,t})}\right]^2\right) \quad \text{with} \quad j = 1, \dots, J \tag{32}$$

$$\text{logit}(\overset{s}{q}_{x,a,t})^{(j)} \sim \mathcal{N}\left(\text{logit}(\overset{s}{\hat{q}}_{x,a,t}), \left[\frac{\hat{\sigma}_{q^{s}_{x,a,t}}}{\overset{s}{\hat{q}}_{x,a,t} \cdot (1 - \overset{s}{\hat{q}}_{x,a,t})}\right]^2\right) \quad \text{with} \quad j = 1, \dots, J \tag{33}$$

where J denotes the number of simulated probabilities from the statistical distribution, $\text{logit}(\overset{s}{q}_{x,a,t})^{j}$ indicates the $j - th$ simulated value in the random sample and $\left[\frac{\hat{\sigma}_{q^{s}_{x,a,t}}}{\overset{s}{\hat{q}}_{x,a,t} \cdot (1 - \overset{s}{\hat{q}}_{x,a,t})}\right]^2$ is the variance of $\text{logit}(\overset{s}{\hat{q}}_{x,a,t})$ calculated using the Delta Method (see Van der Vaart (2000) for details). The quantity $\overset{2}{\hat{\sigma}}_{q^{s}_{x,a,t}}$ indicates the variance of the subnational death probability estimates from US mortality database. An identical notation is employed for the subnational death probability for children aged $0 - 4$ $(q_{0,a,t})$.

Afterwards, we transform the previous simulated values into the original scale. From the simulated samples of death probabilities by age group x, time t, county a and sex s

$$\begin{gathered} \overset{(1)}{q}_{0,a,t}, \dots, \overset{(j)}{q}_{0,a,t}, \dots, \overset{(J)}{q}_{0,a,t} \\ \overset{s(1)}{q}_{x,a,t}, \dots, \overset{s(j)}{q}_{x,a,t}, \dots, \overset{s(J)}{q}_{x,a,t} \end{gathered} \tag{34}$$

we employ standard life table relationships to obtain samples of the simulated Person-Years by age group x, sex s, area a and time t.

$$\begin{aligned} &\tilde{L}^{(1)}_{0,a,t}, \dots, \tilde{L}^{(j)}_{0,a,t}, \dots, \tilde{L}^{(J)}_{0,a,t} \\ &\tilde{L}^{s(1)}_{x,a,t}, \dots, \tilde{L}^{s(j)}_{x,a,t}, \dots, \tilde{L}^{s(J)}_{x,a,t} \end{aligned} \tag{35}$$

In order to estimate the uncertainty around the Person-Years estimates, we calculate the empirical variance of the Person-Years values for each combination of time t, sex s, age group x and area a. Hence, $\hat{\sigma}^2_{\hat{L}_{0,a,t}}$ and $\hat{\sigma}^2_{\hat{L}^s_{x,a,t}}$ are estimated as

$$\hat{\sigma}^2_{\hat{L}_{0,a,t}} = \frac{\sum_{j=1}^{J} \left(\tilde{L}^{(j)}_{0,a,t} - \bar{\tilde{L}}_{0,a,t} \right)^2}{J} \tag{36}$$

$$\hat{\sigma}^2_{\hat{L}^s_{x,a,t}} = \frac{\sum_{j=1}^{J} \left(\tilde{L}^{s(j)}_{x,a,t} - \bar{\tilde{L}}^s_{x,a,t} \right)^2}{J} \tag{37}$$

where $\bar{\tilde{L}}_{0,a,t} = \frac{\sum_{j=1}^{J} \tilde{L}^{(j)}_{0,a,t}}{J}$ and $\bar{\tilde{L}}^s_{x,a,t} = \frac{\sum_{j=1}^{J} \tilde{L}^{s(j)}_{x,a,t}}{J}$ are the empirical averages of the simulated Person-Years estimates.

For our U.S. example, we simulate $J = 1,000$ values for the Person-Years for each combination of age group x, sex s, county a and time t.

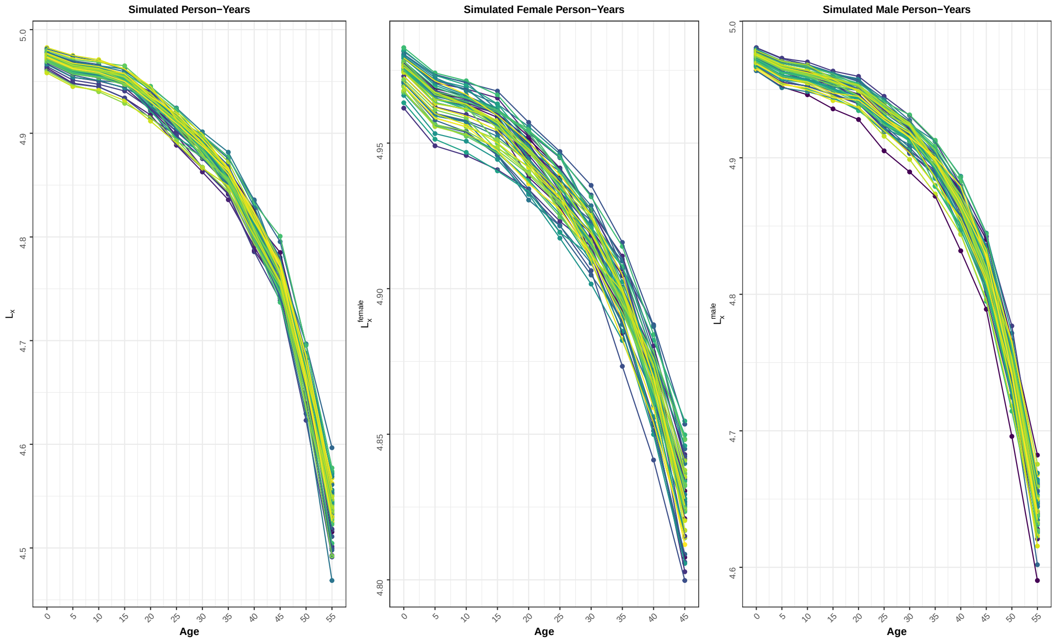

Figure A1: $J = 50$ simulated Person-Years trajectories for Calaveras County in California in year 2000. Simulations are reported for the whole population of the county and by sex.

In figure A1, we show 50 simulated Person-Years estimates for Calaveras County in California in year 2000 by age group x and sex s. Given that this county is characterized by a relatively small population (roughly $46,000$ in 2019), we observe some variations in the simulated Person-Years trajectories. Counties with high population sizes present almost no variation in the simulated Person-Years trajectories. As a consequence, the uncertainty around the Person-Year estimates from these counties will be very tiny.

Details on Data Sources

Information	**Content**	**Period**	**Geographical Detail**	**Source**
Female fertility	Fertility indicators	1933-2021	US country	Human Fertility Database (link)
Male fertility	Fertility indicators	1969-2015	US country	Human Fertility Collection
Mortality	Life tables	1982-2019	US counties	US Mortality Database (link)
Fertility	Birth records	1969-2004	US states	US National Bureau of Economic Research (link)
Population	Population counts by age and sex	1969-2021	US counties	National Cancer Institute (link)
Female fertility	Births by maternal ages	1975-2023	Australian regions	Australian Bureau of Statistics (link)
Male fertility	Births by paternal ages	1975-2023	Australian regions	Australian Bureau of Statistics (link)
Population	Population counts by age and sex	1975-2023	Australian regions	Australian Bureau of Statistics (link)
Mortality	Life tables	2001-2020	Australian regions	Human Life-Table Database (link)

Table A1: Summary of the data sources

Additional Figures

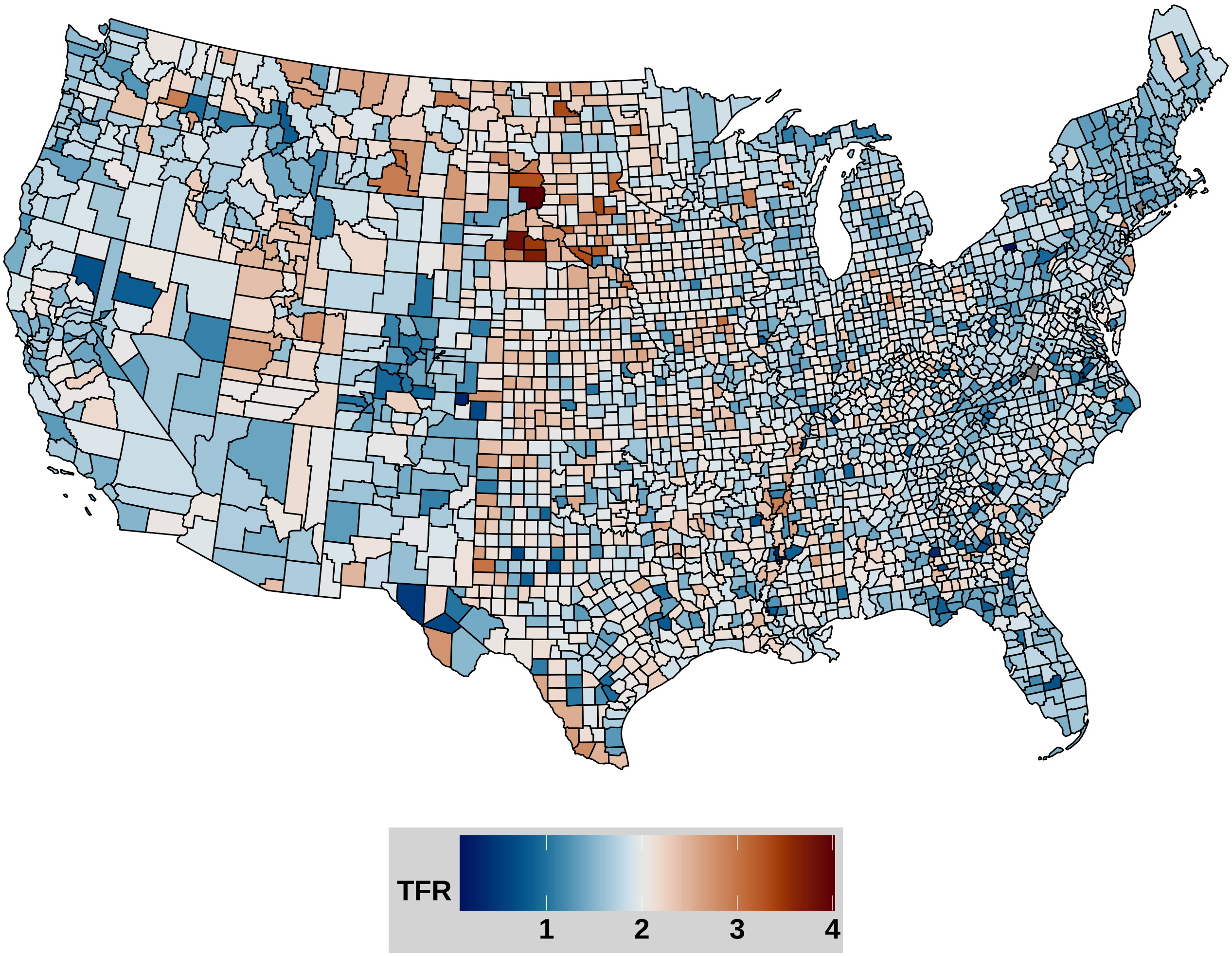

Figure A2: Spatial distribution of male TFR in 2019. Note that only continental counties are displayed.

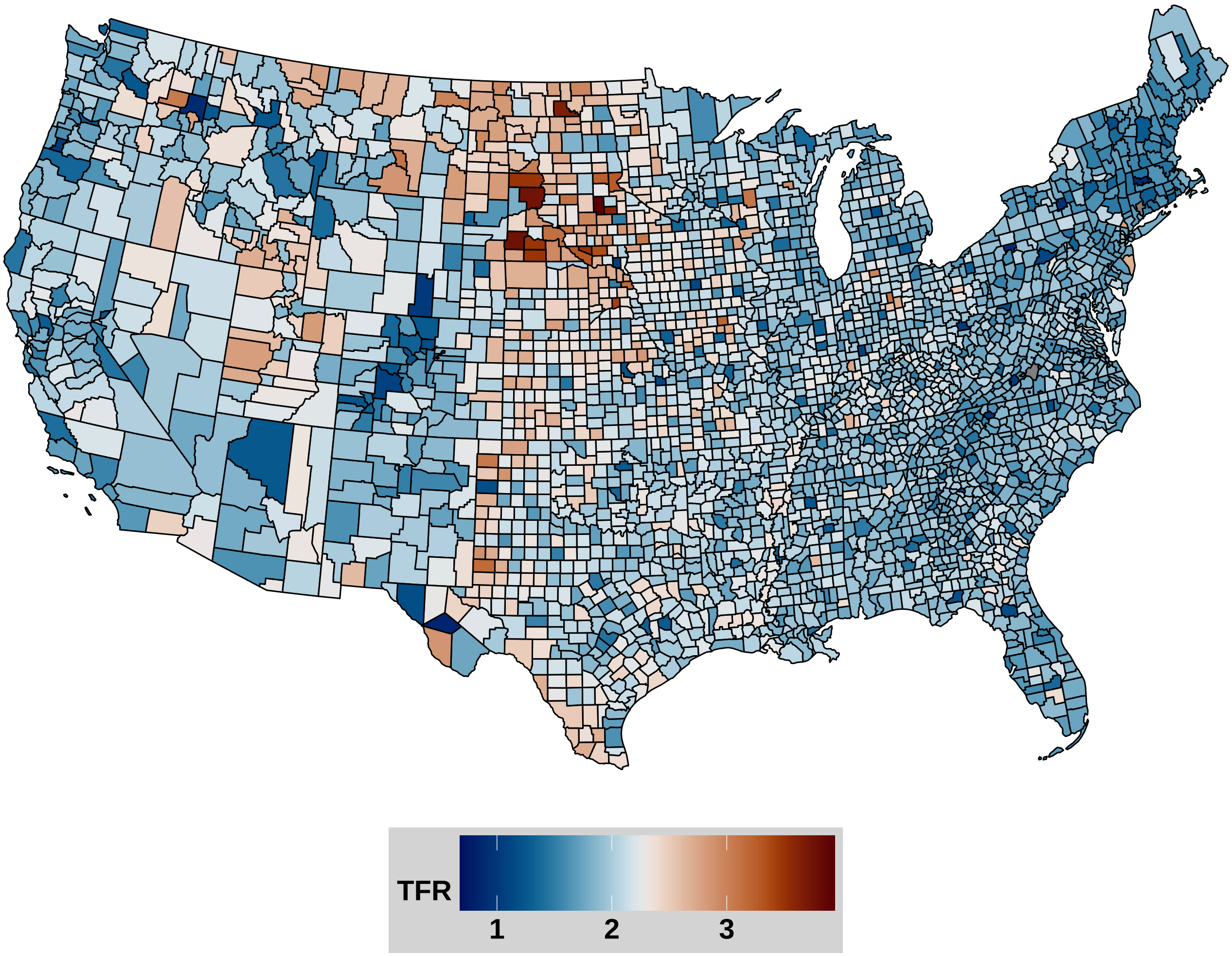

Figure A3: Spatial distribution of female TFR in 2019. Note that only continental counties are displayed.

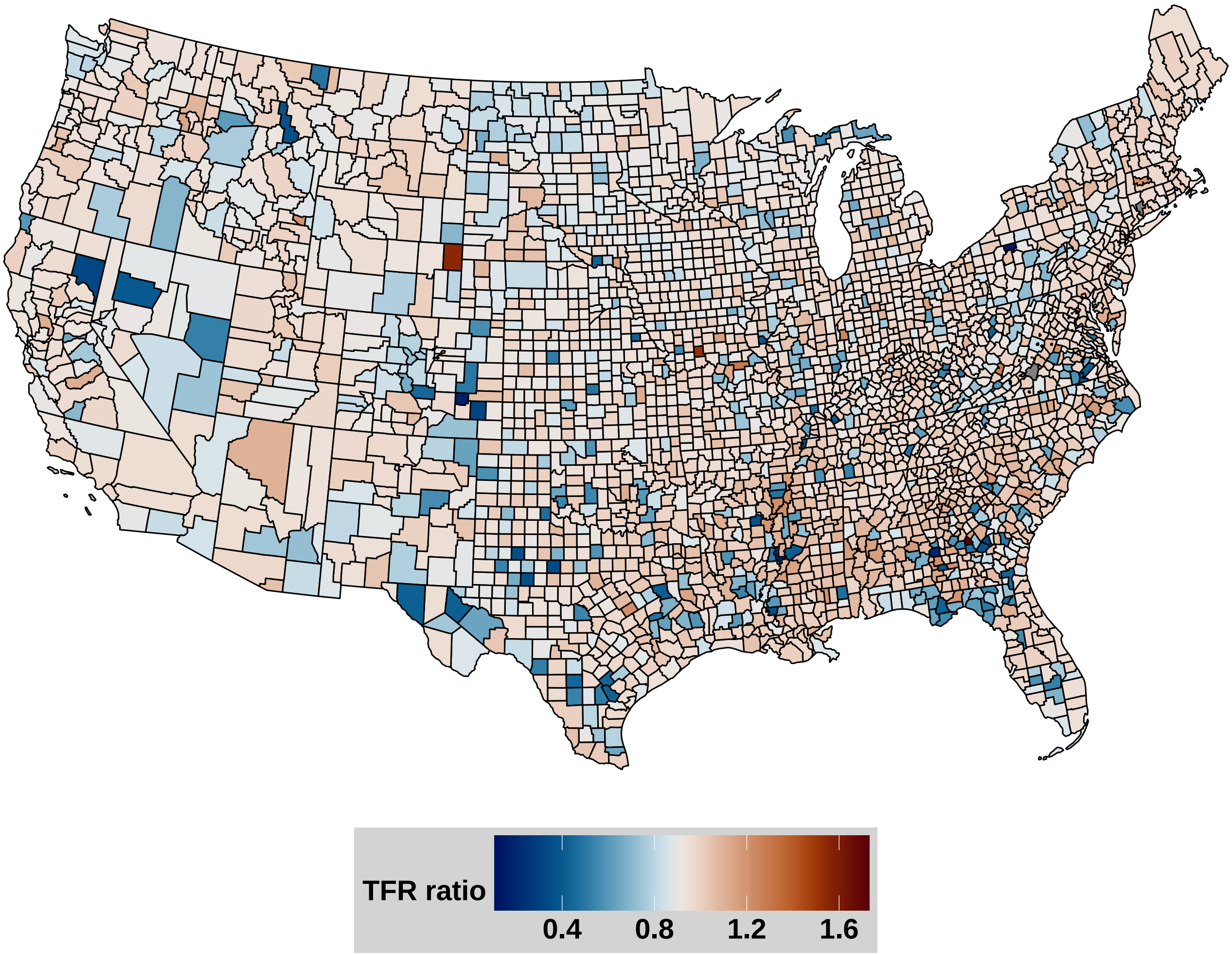

Figure A4: Spatial distribution of the ratio of male TFR to female TFR in 2019. Note that only continental counties are displayed. Values great than 1 denote higher TFR among men, whereas values less than 1 indicate higher TFR among women.